

SAR and Temperature in A Human Head Exposed to 7T High-Pass and Low-Pass Birdcage MRI Coils

Z. Wang¹, J. C. Lin¹

¹University of Illinois-Chicago, Chicago, IL, United States

Introduction

The demand for increased resolution and high signal-to-noise ratio (SNR) from MRI instruments has prompted the use of higher magnetic fields, which also have led to the use of higher levels of radio frequencies and powers. SAR is a widely used metric to quantify the RF energy absorbed inside an object. A major fraction of the absorbed RF energy is converted to heat inside body tissues. While SAR can serve as the driving source of tissue temperature elevation, it cannot account for the exact description of thermal phenomena. The rise in tissue temperature is influenced not only by the power dissipated in the local tissue, but also by the thermal characteristics of the surrounding tissues, and heat exchange with the external environment. Some studies have been reported SAR distribution and temperature calculation during MRI scans^[1,2]. However, they often used ideal current distributions for the coil model and did not consider the convection cooling from the environment. In this paper, we investigate the SAR and temperature distributions in human head, loading high-pass and low-pass 7T birdcage coils with idealized current distributions, two-port and four-port excitations.

Method

The FDTD method is used for modeling the birdcage coil and for studying the interaction between EM fields and human-head models. The computational domain has 160x160x160 grid with 3mmx3mmx3mm cells. An eight-layer Berenger's PML is adopted as the absorption boundary. The human head model, 3mm resolution, was obtained from the Brooks Air Force Laboratories, Brooks AFB, TX. All coil components, including coil elements (wires), lumped capacitors, and the sources, were geometrically modeled. As such, the interaction within the birdcage coil, including the interaction of coil, source, and object (human head) was accurately computed.

The temperature distribution was computed process using Pennes Bio-heat equation, which accounts for such heat exchange mechanisms as heat conduction, blood flow, and EM heating. The Bio-heat equation is given by $\rho C_p \frac{\partial T}{\partial t} = K \nabla^2 T + \rho \text{SAR} + A_0 - B(T-T_b)$, with the boundary

condition $-K(\frac{\partial T}{\partial n})_s = H(T-T_a)$, where ρ is the tissue density, T is the temperature at time t , C_p is the specific heat, K is the thermal conductivity, B is

a constant related to blood flow, T_b is the blood temperature, T_a is the ambient temperature, n is the unit vector normal to the surfaces of the object, H is the convective heat transfer coefficient, and A_0 means the metabolic heat production, SAR is the input EM heating source into the Bio-heat equation. In order to avoid numerical instability, in the choice of the maximum size of the time step is given by $\Delta t \leq \min_{m \in M} (\frac{2\rho_m C_{pm} \Delta}{12K_m + B_m \Delta^2})$.

Here M is the set of tissues. For the convective heat-transfer coefficient H , two values were used: $H_a=10.5 \text{ W/m}^2 \text{ }^\circ\text{C}$, which is the coefficient from the head surface to the ambient temperature, and $H_b=50 \text{ W/m}^2 \text{ }^\circ\text{C}$, which is the coefficient from the internal surface to the cavity, such as throat, skull etc.

Result and Discussion

In these calculation, the power absorption for the head-with-the-shoulder model was normalized to 20W. Results for the high-pass and low-pass birdcage coils are shown in Fig 1 and Fig 2, respectively. We calculated the temperature change for two hours at different time steps. Note that the temperature increased rapidly in the first 30 min (The temperature rise value at 30 min is about 95% of the value at 2 hrs.), and the rate of temperature rise was then slowed down. The steady-state temperature was reached (no temperature variation at any cells) after two hours. For the high-pass coil, the ideal current distribution gave a $\Delta T_{\text{max}}=1.26^\circ\text{C}$, which is lower than that calculated from the two-port excitation ($\Delta T_{\text{max}}=1.45^\circ\text{C}$) and the four-port excitation ($\Delta T_{\text{max}}=1.45^\circ\text{C}$). The difference in temperature rise is not obvious among these three excitation modes. The maximum temperature rise is around the eye area. This is most likely due to the zero blood flow rate in the aqueous humor, cornea, lens, and sclera, which reduced the ability to convectively cool the region. For the low-pass coil, the ideal current distribution produced a $\Delta T_{\text{max}}=2.52^\circ\text{C}$, which is much lower than that produced by the two-port excitation ($\Delta T_{\text{max}}=5.14^\circ\text{C}$) and the four-port excitation ($\Delta T_{\text{max}}=3.63^\circ\text{C}$). In this case, the temperature rise apparently is different among the three-excitation modes. The maximum temperature rise was in the back of head, within muscle and fat tissues. The higher temperature rise is associated with the high SAR in that region. It is concluded that the performance of the low-pass coil is worse than the high-pass coil in ultra-high field MRI. Moreover, the spatial correlation between SAR and temperature increase is not very good. In fact, the augmented thermal conduction mechanism, due to the presence of a high blood flow rate in the brain, greatly facilitates the amount of heat transfer, and depresses the temperature rise in the upper part of the head. Thus, a thermal analysis is necessary, in addition to SAR analysis, to assess the safety of high field MRI.

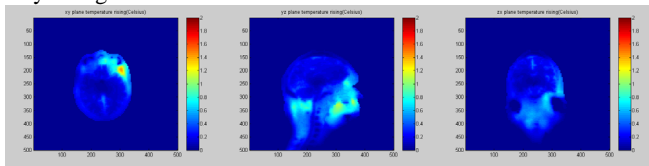


Fig 1

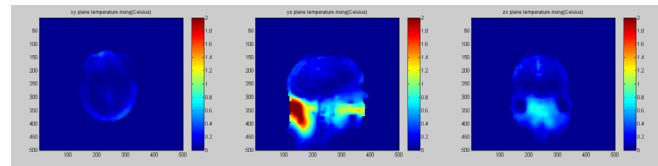


Fig 2

Reference

1. U. D. Nguyen et al, IEEE Biom Eng, 2004;51:1301-1309
2. C. M. Collins et al, J MRI, 2004;19:650-656